Application of a Variational Mode Decomposition-Based Instantaneous Centroid Estimation Method to a Carbonate Reservoir in China

Article *in* IEEE Geoscience and Remote Sensing Letters · January 2018
DOI: 10.1109/LGRS.2017.2788467

6 authors, including:

Ya-juan Xue
Chengdu University of Information Technology
34 PUBLICATIONS **123** CITATIONS

SEE PROFILE

Junxing Cao
Chengdu Institute of Technology
67 PUBLICATIONS **332** CITATIONS

SEE PROFILE

Wei Chen
Yangtze University
37 PUBLICATIONS **182** CITATIONS

SEE PROFILE

Application of a Variational Mode Decomposition-Based Instantaneous Centroid Estimation Method to a Carbonate Reservoir in China

Ya-Juan Xue, Hao-Kun Du, Jun-Xing Cao, Da Jin, Wei Chen, and Juan Zhou

***Abstract*— A novel hydrocarbon detection technique named the variational mode decomposition (VMD)-based instantaneous centroid method is proposed in this letter. It reveals frequency-dependent amplitude anomalies that may reflect some details deeply buried within the intrinsic mode functions (IMFs) in particular frequency bands. Instantaneous amplitude and instantaneous frequency information from each IMF are used to generate each IMF instantaneous centroid. A weighted correlation scheme is employed to generate the VMD-based instantaneous centroid volume for a seismic trace. Model testing and field data from a carbonate reservoir in China illustrate that the VMD-based instantaneous centroid method can provide a better hydrocarbon-prone interpretation with a higher resolution and accuracy. Comparisons between the VMD-based instantaneous centroid method and the short-time Fourier transform, and continuous wavelet transform and prestack wave impedance inversion technology indicate that the proposed method is more convenient and can effectively target gas reservoirs. This letter presents a complementary approach to current methods used to extract frequency-dependent amplitude anomaly information.**

***Index Terms*— Hydrocarbon detection, instantaneous centroid, intrinsic mode function (IMF), seismic interpretation, variational mode decomposition (VMD).**

I. Introduction

IN OIL and gas exploration, there are numerous difficult problems, including how to extract more useful information especially frequency-dependent amplitude anomaly information from the instantaneous attributes of seismic signals and how to combine that information with geological interpretations, logging data, and other information to find meaningful oil and gas reservoirs. The solutions of these obstacles represent long-term goals for petroleum geophysical researchers. Frequency-dependent amplitude anomaly information is widely used for hydrocarbon detection since seismic wave energies exhibit obvious high-frequency attenuation in or beneath gas-bearing layers [1]–[4]. Spectral decomposition is an effective and commonly used geological interpretation and hydrocarbon indication method utilizing seismic reflection data with only high-frequency attenuation anomaly information from seismic signals [5]. Seismic data can produce a series of common frequency volumes via spectral decomposition. Each common frequency volume is a reflection of the instantaneous amplitude of the seismic data at a particular frequency or in a special frequency band. Amplitude volumes at different frequencies can reflect the different response characteristics of geological bodies at different scales, and hydrocarbon information may be enhanced and reflected in the common frequency volumes at some certain frequencies. Hydrocarbon-bearing areas often exhibit attenuation characteristics with strong energies at low frequencies and weak energies at high frequencies [3], [4], [6], [7]. However, spectral decomposition technology requires a series of common frequency volumes for analysis prior to selecting reasonable common frequency volumes for interpretation. The associated workload is heavy.

Variational mode decomposition (VMD) is a newly developed nonrecursive decomposition method for nonlinear and nonstationary signals [8]. It has been proven to demonstrate better local decomposition abilities, higher spectral and spatial resolutions, and better noise robustness than empirical modal decomposition (EMD), as well as the methods derived from EMD and other conventional time–frequency methods [8]–[10]. VMD can decompose a seismic trace into several intrinsic mode functions (IMFs). Different IMFs have different frequency bands. Each IMF may reflect different details of the original seismic signal. In addition, some details may be highlighted in one or more IMFs [11], [12].

The objective of this letter is to introduce a new geological interpretation and hydrocarbon indicator method, that is, the VMD-based instantaneous centroid method, and then demonstrate the ability of this new technique for seismic interpretation. This letter hopes to complement current frequency-dependent methods used to extract amplitude anomaly information with the addition of the VMD-based instantaneous centroid method. First, we outline the principle of the VMD-based instantaneous centroid method. Then, a model

Manuscript received November 28, 2017; accepted December 27, 2017. Date of publication January 17, 2018; date of current version February 23, 2018. This work was supported in part by the National Natural Science Foundation of China under Grant 41404102, Grant 41430323, and Grant 61601064, in part by the Sichuan Youth Science and Technology Foundation under Grant 2016JQ0012, and in part by the Project for Young Scientists Fund of Hubei Ministry of Education under Grant Q20161304. *(Corresponding author: Ya-Juan Xue.)*

Y.-J. Xue and J. Zhou are with the School of Communication Engineering, Chengdu University of Information Technology, Chengdu 610225, China (e-mail: xueyj0869@163.com).

H.-K. Du and D. Jin are with the Geophysical Institute of Zhongyuan Oilfield, Sinopec, Henan 457000, China.

J.-X. Cao is with the State Key Laboratory of Oil and Gas Reservoir Geology and Exploitation, Chengdu University of Technology, Chengdu 610059, China.

W. Chen is with the Key Laboratory of Exploration Technology for Oil and Gas Resources of Ministry of Education, Yangtze University, Wuhan 430100, China.

Color versions of one or more of the figures in this letter are available online at http://ieeexplore.ieee.org.

Digital Object Identifier 10.1109/LGRS.2017.2788467

test is used to evaluate the effectiveness of the VMD-based instantaneous centroid method. Finally, a field data application is carried out to study the characteristics of the proposed method and evaluate its effectiveness.

II. Principle and Methods

A. Variational Mode Decomposition

VMD can decompose a seismic signal $x(t)$ into several numbers of IMFs as defined in

$$u_k(t) = A_k(t)\cos(\phi_k(t)) \tag{1}$$

where t is the time variable, and $A_k(t) \geq 0$, $\phi_k'(t) \geq 0$, $A_k(t)$, and $\phi_k'(t)$ vary much more slowly than $\phi_k(t)$. Such a more restrictive definition ensures that each IMF $u_k(t)$, which is a pure harmonic signal with an amplitude $A_k(t)$ and instantaneous frequency $\phi_k'(t)$, has a sufficiently long interval. Each IMF exhibits a narrow-band property that maintains the physical meaning of the resulting instantaneous frequency.

VMD is a constrained variational problem that is described as follows [8]:

$$\min_{\{u_k\},\{\omega_k\}} \left\{ \sum_k \left\| \partial_t \left[\left(\delta(t) + \frac{j}{\pi t} \right) * u_k(t) \right] e^{-j\omega_k t} \right\|_2^2 \right\}$$
$$\text{s.t.} \sum_k u_k = x \tag{2}$$

where $*$ represents a convolution calculation and $\delta(t)$ is the Dirac distribution. Here, each mode u_k is mostly compact around a center frequency ω_k. A quadratic penalty term and Lagrangian multipliers λ are employed to make (2) unconstrained. The augmented Lagrangian L is given by the following equation:

$$\begin{aligned} L(u_k, \omega_k, \lambda) &= \alpha \sum_k \left\| \partial_t \left[\left(\delta(t) + \frac{j}{\pi t} \right) * u_k(t) \right] e^{-j\omega_k t} \right\|_2^2 \\ &\quad + \left\| x(t) - \sum u_k(t) \right\|_2^2 + \left\langle \lambda(t), x(t) - \sum u_k(t) \right\rangle \end{aligned} \tag{3}$$

where α is the balancing parameter of the data-fidelity constraint.

The variational problem in (3) is solved using an alternate direction method of multipliers (ADMM) approach. Then, the center frequency and different decomposed modes are produced via the ADMM approach during each shifting process. The obtained mode $u_k(t)$ in the time domain can be represented as

$$\hat{u}_k(\omega) = \frac{\hat{x}(\omega) - \sum_{i!=k} \hat{u}_i(\omega) + (\hat{\lambda}(\omega)/2)}{1 + 2\alpha(\omega - \omega_k)^2} \tag{4}$$

$$\hat{u}_k(t) = R\{\text{ifft}(\hat{u}_k(\omega))\} \tag{5}$$

where $\hat{x}(\omega)$ is the Fourier transform of $x(t)$. ifft$(\cdot)$ denotes the inverse Fourier transform of the signal and $R(\cdot)$ represents the real part of an analytic signal. Note that the optimal $u_k(\omega)$ is updated directly through Wiener filtering in the Fourier domain. In addition, the fact that Wiener filtering is embedded within the VMD approach makes it more robust to noise and sampling.

The center frequencies ω_k^{n+1} are updated as follows:

$$\omega_k^{n+1} = \frac{\int_0^\infty \omega \left| \hat{u}_k^{n+1}(\omega) \right|^2 d\omega}{\int_0^\infty \left| \hat{u}_k^{n+1}(\omega) \right|^2 d\omega}. \tag{6}$$

For all $\omega \geq 0$, the exact reconstructed signal is obtained through a dual ascent, that is, the updated Lagrangian multiplier $\hat{\lambda}^{n+1}$ shown in

$$\hat{\lambda}^{n+1} = \hat{\lambda}^n + \tau \left(\hat{f} - \sum_k \hat{u}_k^{n+1} \right) \tag{7}$$

until $\sum_k \|\hat{u}_k^{n+1} - \hat{u}_k^n\|_2^2 / \|\hat{u}_k^n\|_2^2 < \varepsilon$.

A detailed description of the VMD algorithm can be found in [8].

B. Principle of the VMD-Based Instantaneous Centroid Method

For each IMF $u(t)$ obtained following the application of VMD, its instantaneous amplitude $A(t)$, instantaneous phase $\varphi(t)$, and instantaneous frequency $f(t)$ can be computed using the following equation:

$$\begin{cases} A(t) = \sqrt{u^2(t) + y^2(t)} \\ \varphi(t) = \arctan(y(t)/u(t)) \\ f(t) = \dfrac{1}{2\pi} \dfrac{d\varphi(t)}{dt} \end{cases} \tag{8}$$

where $y(t)$ is the Hilbert transform of the IMF $u(t)$.

Generally, to avoid ambiguities caused by phase unwrapping in (8), the instantaneous frequency $f(t)$ can be computed as follows:

$$f(t) = \frac{1}{2\pi} \frac{u(t)\frac{dy(t)}{dt} - \frac{du(t)}{dt} y(t)}{u^2(t) + y^2(t)}. \tag{9}$$

If N IMFs are generated by applying VMD to a seismic trace $x(t)$, let $c_k(t)$ be the corresponding seismic instantaneous centroid of each IMF $u_k(t)(k = 1 \sim N)$. The instantaneous centroid of an IMF is written as

$$c_k(t) = \frac{A_k(t) f_k(t)}{\sum A_k(t)}. \tag{10}$$

The IMF-based instantaneous centroid $c_k(t)$ is a frequency-dependent amplitude attribute that may highlight some details deeply buried within the IMFs at particular frequency bands. A meaningful instantaneous frequency calculated from an IMF ensures that the seismic instantaneous centroid $c_k(t)$ has a physical meaning and can reveal geological information effectively. Then, the seismic instantaneous centroid of a trace $C(t)$ can be generated via the following equation:

$$C(t) = \sum_{k=1}^{N} R_c \cdot c_k(t) \tag{11}$$

where R_c [as defined in (12)] is a weighted correlation coefficient, and R denotes the correlation coefficient between the IMF $u_k(t)$ and the original seismic trace $x(t)$.

$$R_c = \begin{cases} 1, & |R| \geq 0.3 \\ 10^{-1}, & 0.1 \leq |R| < 0.3 \\ 10^{-2}, & |R| \leq 0.1 \end{cases} \tag{12}$$

As shown in (12), R_c remains the instantaneous centroid of the mode that has the strongest correlation with the original

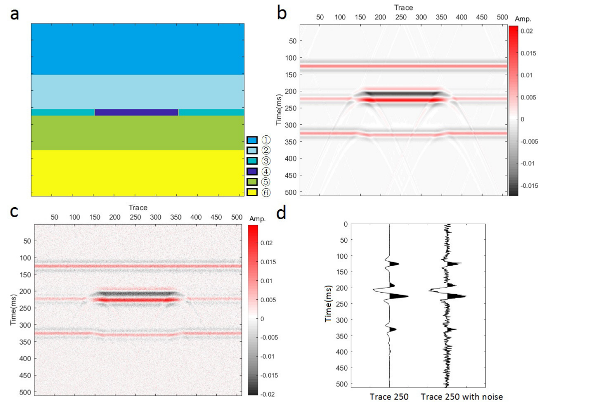

Fig. 1. (a) Geological model. (b) Its seismic response. (c) Synthetic data with noise. (d) Comparison with the trace.

seismic trace unchanged, attenuates the instantaneous centroid of the mode that has a stronger correlation with the original seismic trace with a coefficient of 10^{-1}, and attenuates the instantaneous centroid of the mode that has the weakest correlation with a coefficient of 10^{-2}. This operation aims to strengthen the main contributors of the seismic trace and weaken the other less important information.

Finally, we apply a normalization operation to the seismic instantaneous centroid $C(t)$ and make the values distributed in the range [0, 1]. This operation ensures that the lateral changes among different traces will not be excessively large. We can obtain a seismic instantaneous centroid volume by calculating $C(t)$ trace by trace.

Note that although many studies have illustrated the decomposition level of VMD for many fields [8], [15]–[17], these decomposition level choosing methods do not work for hydrocarbon detection. In this letter, we use an empirical expression to determine the decomposition level k of VMD

$$k = \left[\frac{f_s/f_{\text{domi}}}{\log(N)}\right] - 1 \tag{13}$$

where f_{domi} is the dominant frequency of each seismic trace, f_s is the sampling frequency, N is the length of each seismic trace, and $[\cdot]$ denotes a rounding up operation.

III. Model Test

In this section, we produce a model to simulate the seismic response using the 3-D diffusive-viscous wave equation [13], [14] to validate the effectiveness of the VMD-based instantaneous centroid estimation method.

We design the geological model based on reservoir logging parameters and seismic data from a marine carbonate reservoir in the Puguang gas field, Sichuan Basin, China. The geological model is shown in Fig. 1(a). The parameters of the six layers in the model are shown in Table I. The frequency of the wavelet is 25 Hz. The seismic data are sampled at an interval of 1 ms. A highly permeable gas-bearing reservoir is denoted by the layer marked ④ with a thickness of 40 m and its adjoining dry layer is marked as ③. The seismic response of the model is shown in Fig. 1(b).

The IMF-based instantaneous centroid results using the VMD method after the modeling are shown in Fig. 2(a). Note that the VMD decomposition level is set to 5. As shown in Fig. 2(a), strong amplitude anomalies are found in the gas layer marked ④.

TABLE I

Rock Properties for the Geological Model

Layer number	V_p $(m \cdot s^{-1})$	ρ $(g \cdot cm^{-3})$	ζ (Hz)	η $(m^2 \cdot s^{-1})$	Q
①	5975	2.78	1.0	1.0	200
②	6274	2.72	1.0	1.0	200
③	6428	2.74	1.0	1.0	200
④	6052	2.52	10	500	5
⑤	6306	2.79	1.0	1.0	200
⑥	6488	2.76	1.0	1.0	200

Note that ζ is the diffusion coefficient. η is the viscous coefficient.

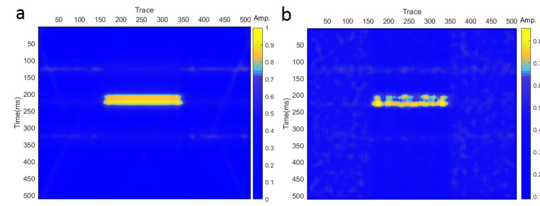

Fig. 2. (a) VMD-based instantaneous centroid estimation method after the model test. (b) Model with noise. The VMD decomposition level is set to five.

To further validate the effectiveness of the proposed method, we add some noise to the model. The signal-to-noise ratio is set to 55 dB. The synthetic data with noise are shown in Fig. 1(c). Fig. 1(d) shows a comparison between trace 250 and trace 250 with noise. The corresponding VMD-based instantaneous centroid section shown in Fig. 2(b) also shows a strong amplitude anomaly in the gas layer marked ④. The proposed method can therefore target a gas layer accurately.

The model test shows that the VMD-based instantaneous centroid estimation method can effectively target the reservoir and demonstrates some noise robustness.

IV. Field Data

A. Study Area Setting

In this section, we apply the VMD-based instantaneous centroid estimation method to the broadband migrated and stacked seismic data from the Puguang gas field, Sichuan Basin, China, to evaluate the validity of our approach.

The Puguang gas field is mainly composed of carbonate reservoirs. We mainly study one major producing gas reservoir distributed throughout the first–second section of the Feixianguan section, Lower Triassic. The reservoir type mainly comprises a platform margin oolitic bank, typically containing high-porosity, high-permeability, and high-abundance lithologic gas reservoir traps. The average porosity of the first–second section is 8.89%, and the average permeability is $143.813 \times 10^{-3}\ \mu\text{m}^2$.

We first use one stacked 2-D seismic section intersecting a known prolific gas well (well A) to give a detailed example and illustrate the feasibility and accuracy of the proposed method. For comparison, we also provide results from prestack wave impedance inversion and spectrum decomposition results using conventional time–frequency methods on the stacked seismic data. Then, 3-D seismic data are used for an analysis.

B. Two-Dimensional Seismic Data Processing

The broadband migrated and stacked seismic section intersecting the target layer in well A, a known prolific gas well,

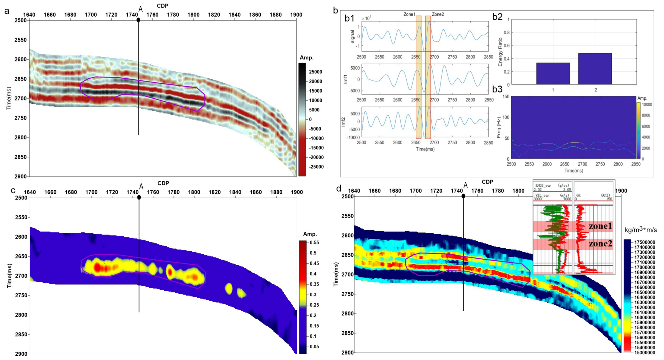

Fig. 3. (a) Seismic section intersecting well A. (b1) Seismic trace intersecting well A and its corresponding IMFs obtained using VMD. The VMD decomposition level is set to 2. (b2) Energy ratio of the energy of each IMF to the original seismic trace energy. (b3) Time–frequency spectrum after VMD. (c) Its corresponding IMF-based instantaneous centroid section intersecting well A using the VMD method. (d) Prestack wave impedance inversion section intersecting well A. Only the seismic data between the two horizontal lines are displayed. The area where well A is located and good gas production is obtained is delineated by a pink polygon. Note that the interpretation of the target layer in well A is also shown.

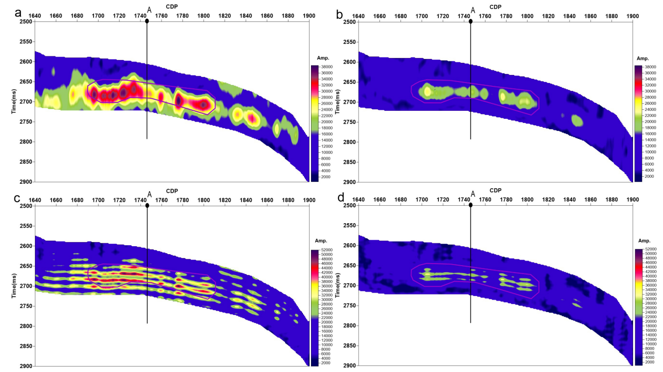

Fig. 4. (a) Common frequency sections after applying the STFT at 30 Hz. (b) Common frequency sections after applying the STFT at 45 Hz. (c) Common frequency sections after applying the CWT at 30 Hz. (d) Common frequency sections after applying the CWT at 45 Hz. Note that a Morlet wavelet is used for the CWT and a Hamming window with a length of 41 is used for the STFT.

is illustrated in Fig. 3(a). We analyze only the 2-D broadband migrated and stacked seismic section intersecting the target layer in well A between two horizons as shown in Fig. 3(a) to exclude the lithology and other factors that could lead to the ambiguities in the hydrocarbon interpretation using the proposed method. Because the reservoir type mainly comprises a platform margin oolitic bank in the target layer, only a relatively simple structure without cracks and marlite is shown in the target layer. The area where well A is located and good gas production is obtained is delineated by a pink polygon. The seismic signals are sampled at an interval of 2 ms.

We first analyze the seismic trace intersecting well A. Fig. 3(b1) shows the seismic trace intersecting well A and its corresponding IMFs obtained using VMD. We mark the two reservoir areas as zone 1 and zone 2. We find that the differences between the areas where the reservoirs are located and their surrounding area are more obvious in the second IMF, meaning that hydrocarbon-related information is reflected more greatly in this subsignal. The energy ratio of the energies of the two obtained IMFs to the original seismic trace is shown in Fig. 3(b2). Both IMFs have larger energies, and the energy of the second IMF is larger than that of the first. The time–frequency spectrum for the seismic trace after VMD is shown in Fig. 3(b3), which shows that the main frequency range of the seismic trace is approximately 0–50 Hz. We can also find that stronger energy is distributed at times from approximately 2650 to 2700 ms, which is where the reservoir is located. Moreover, the post-VMD time–frequency spectrum of the seismic trace intersecting well A has a high time–frequency resolution. Consequently, the VMD-based instantaneous centroid estimation method is applied to the seismic section [Fig. 3(c)]. As shown in Fig. 3(c), strong anomalous amplitudes are found in the reservoirs delineated by the pink polygon. Fig. 3(d) shows the corresponding prestack wave impedance inversion section intersecting well A. Note that the interpretation of the target layer in well A is also shown in Fig. 3(d). The two gas-bearing layers are marked by zone 1 and zone 2 in the well interpretation map. In addition, their corresponding areas are marked with two arrows in the prestack wave impedance inversion section. Since the area of the reservoir obtained using the prestack wave impedance inversion section in Fig. 3(d) is consistent with the reservoir area in the IMF-based instantaneous centroid section using the VMD method in Fig. 3(c), the proposed method can effectively interpret hydrocarbon-prone areas.

Fig. 4 shows the common frequency sections after spectrum decomposition using the conventional short-time Fourier transform (STFT) and continuous wavelet transform (CWT). Strong anomalous amplitudes are found in the area delineated by the pink polygon in the lower common frequency sections (30 Hz) for using both the STFT and the CWT [Fig. 4(a) and (c)]. However, they are all weakened in the higher common frequency sections (45 Hz) for both the STFT and the CWT [Fig. 4(b) and (d)]. Both the STFT and the CWT give hydrocarbon-prone interpretations. However, comparing the results obtained after employing the proposed method in Fig. 3(c) with the results in Fig. 4, the VMD-based instantaneous centroid section has higher temporal and spatial resolutions than those obtained using the conventional spectrum decomposition methods in Fig. 4. Furthermore, the proposed method is more convenient in that it is unlike conventional spectrum decomposition methods that must analyze a series of common frequency volumes to provide suitable interpretation results.

C. Three-Dimensional Seismic Data Processing

In this section, we apply the proposed VMD-based instantaneous centroid estimation method to the 3-D broadband migrated and stacked seismic data from the Puguang gas field. Here, except and in addition to a prolific gas well (well A), another three other wells, respectively, named B, C, and D are also located in this area. Well C is the most prolific gas well. Well B is a prolific gas and water well. Well D is a water well. Fig. 5(a) shows the time slice at the target layer, and the results after applying the proposed VMD-based instantaneous centroid estimation method to the 3-D broadband migrated stacked seismic data are shown in Fig. 5(b). As shown in Fig. 5(b), strong amplitude anomalies are found in the area where wells B and C are located. Less strong weaker amplitude anomalies exist in the area where well A is located. The area where well D is located has the weakest least amplitude anomalies. The consistency between the well

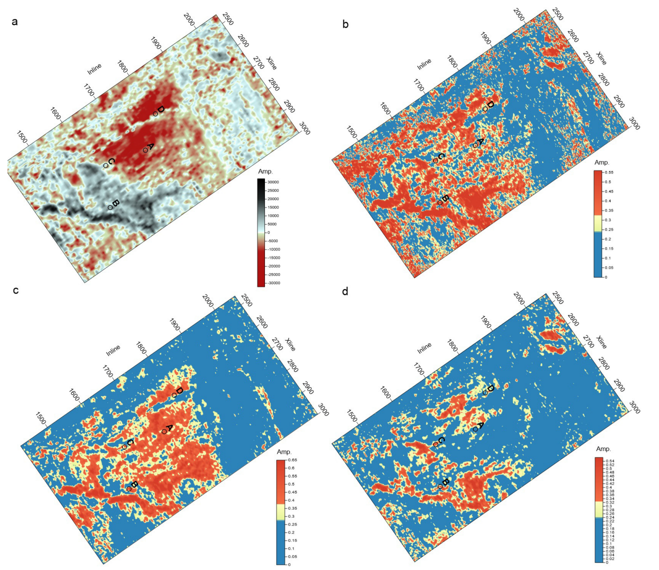

Fig. 5. (a) Time slice at the target layer. (b) Results after employing the proposed VMD-based instantaneous centroid estimation method. The VMD decomposition level is set to two. (c) Results after employing the spectral decomposition method using the STFT at 30 Hz. (d) Results after employing the spectral decomposition method using the STFT at 45 Hz.

testing data and the analysis results after applying the proposed VMD-based instantaneous centroid estimation method to the 3-D broadband migrated and stacked seismic data indicates that the use of the proposed method in the area can effectively provide a hydrocarbon-prone interpretation effectively and reliably predict the favorable gas zones well in the study area. In comparison, the spectral decomposition results after applying the STFT at different frequencies are also shown in Fig. 5(c) and (d). We find that strong amplitude anomalies exist in the areas where the wells are located at 30 Hz. The amplitudes around wells A and D decay obviously at 45 Hz. However, this amplitude attenuation does not exist for wells B and C in the common frequency slices at 45 Hz. These results provide poorer hydrocarbon-prone interpretations for wells B and C. Meanwhile, the proposed method shows higher temporal and spatial resolutions and does not require a series of common frequency sections for interpretation.

V. Conclusion

In this letter, we have presented a novel hydrocarbon detection method approach named the VMD-based instantaneous centroid method for displaying to display frequency-dependent amplitude anomalies. This method is capable of highlighting some details that are deeply buried in the IMFs with in particular frequency bands. The following conclusions are drawn based on the theoretical analysis and practical application.

1) Compared with the conventional spectral decomposition methods, the VMD-based instantaneous centroid method can reveal frequency-dependent amplitude anomalies using the amplitude information combined with the frequency information of from each IMF to give a frequency-dependent amplitude anomaly display. The proposed method is more convenient than other methods. It is unlikely that the conventional spectrum decomposition methods need a series of common frequency volumes to provide a seismic interpretation.
2) A weighted correlation scheme is taken to generate the VMD-based instantaneous centroid volume for a seismic trace. This operation hopes to improve the useful information and details of a seismic trace, and weakens the less useful information. An empirical expression is employed to determine the decomposition level based on the model test, and two field examples are given.
3) A model test and field data applications show that the VMD-based instantaneous centroid estimation method gives a better hydrocarbon-prone-related interpretation with a higher resolution and accuracy.

Acknowledgment

The authors would like to thank the SINOPEC Key Laboratory of Geophysics for their support.

References

[1] A. L. Anderson and L. D. Hampton, "Acoustics of gas-bearing sediments I. Background," *J. Acoust. Soc. Amer.*, vol. 67, no. 6, pp. 1865–1889, Jun. 1980.

[2] S. Maultzsch, M. Chapman, E. Liu, and X.-Y. Li, "Modelling and analysis of attenuation anisotropy in multi-azimuth VSP data from the Clair field," *Geophys. Prospecting*, vol. 55, no. 5, pp. 627–642. Aug. 2007.

[3] M. J. Duchesne, E. J. Halliday, and J. V. Barrie, "Analyzing seismic imagery in the time–amplitude and time–frequency domains to determine fluid nature and migration pathways: A case study from the Queen Charlotte Basin, offshore British Columbia," *J. Appl. Geophys.*, vol. 73, no. 2, pp. 111–120, Feb. 2011.

[4] Y.-J. Xue, J.-X. Cao, R.-F. Tian, H.-K. Du, and Y.-X. Shu, "Application of the empirical mode decomposition and wavelet transform to seismic reflection frequency attenuation analysis," *J. Petroleum Sci. Eng.*, vol. 122, pp. 360–370, Oct. 2014.

[5] J. P. Castagna, S. Sun, and R. W. Siegfried, "Instantaneous spectral analysis: Detection of low-frequency shadows associated with hydrocarbons," *Leading Edge*, vol. 2, pp. 120–127, Feb. 2003.

[6] D. Ebrom, "The low-frequency gas shadow on seismic sections," *Leading Edge*, vol. 23, no. 8, p. 772, Aug. 2004.

[7] M. T. Taner, F. Koehler, and R. E. Sheriff, "Complex seismic trace analysis," *Geophysics*, vol. 44, no. 6, pp. 1041–1063, Jun. 1979.

[8] K. Dragomiretskiy and D. Zosso, "Variational mode decomposition," *IEEE Trans. Signal Process.*, vol. 62, no. 3, pp. 531–544, Feb. 2014.

[9] W. Liu, S. Cao, Z. Wang, X. Kong, and Y. Chen, "Spectral decomposition for hydrocarbon detection based on VMD and Teager–Kaiser energy," *IEEE Geosci. Remote Sens. Lett.*, vol. 14, no. 4, pp. 539–543, Feb. 2017.

[10] Y.-J. Xue, J.-X. Cao, D.-X. Wang, H.-K. Du, and Y. Yao, "Application of the variational-mode decomposition for seismic time–frequency analysis," *IEEE J. Sel. Topics Appl. Earth Observ. Remote Sens.*, vol. 9, no. 8, pp. 3821–3831, Mar. 2016.

[11] S. Yu and J. Ma, "Complex variational mode decomposition for slop-preserving denoising," *IEEE Trans. Geosci. Remote Sens.*, vol. 56, no. 1, pp. 586–597, Jan. 2018, doi: 10.1109/TGRS.2017.2751642.

[12] F. Li, B. Zhang, R. Zhai, H. Zhou, and K. J. Marfurt, "Depositional sequence characterization based on seismic variational mode decomposition," *Interpretation*, vol. 5, no. 2, pp. SE97–SE106, Apr. 2017.

[13] V. A. Korneev, G. M. Goloshubin, T. M. Daley, and D. B. Silin, "Seismic low-frequency effects in monitoring fluid-saturated reservoirs," *Geophysics*, vol. 69, no. 2, pp. 522–532, Mar. 2004.

[14] X.-H. Chen, Z.-H. He, and W.-L. Zhong, "Numeric simulation in the relationship between low frequency shadow and reservoir characteristic," *J. China Univ. Mining Technol.*, vol. 40, no. 4, pp. 584–591, Aug. 2011.

[15] S. Lahmiri and M. Boukadoum, "Biomedical image denoising using variational mode decomposition," in *Proc. IEEE Biomed. Circuits Syst. Conf. (BioCAS)*, Oct. 2014, pp. 340–343.

[16] Y. Wang, R. Markert, J. Xiang, and W. Zheng, "Research on variational mode decomposition and its application in detecting rub-impact fault of the rotor system," *Mech. Syst. Signal Process.*, vols. 60–61, pp. 243–251 Aug. 2015.

[17] Y. Liu, G. Yang, M. Li, and H. Yin, "Variational mode decomposition denoising combined the detrended fluctuation analysis," *Signal Process.*, vol. 125, pp. 349–364, Aug. 2016.